2023 IEEE/ASME International Conference on Advanced Intelligent Mechatronics (AIM)
June 28-30, 2023. Seattle, Washington, USA

A Reliable Kinematic Measurement of Upper Limb Exoskeleton for VR Therapy with Visual-inertial Sensors

Thomas M. Kwok
Integrative Sciences and Engineering Programme, NUS Graduate School
National University of Singapore
Singapore
thomasm.kwok@u.nus.edu

Tong Li
Dept. of Biomedical Engineering
National University of Singapore
Singapore
tong.li@nus.edu.sg

Haoyong Yu
Dept. of Biomedical Engineering
National University of Singapore
Singapore
bieyhy@nus.edu.sg

Abstract— **Virtual reality (VR) is a powerful technology that provides a structured and safe environment for ADL training, allowing patients to have a similar experience as real-world training. However, a limited robot sensing system is proven reliable for such training. The effectiveness of current robot sensors was limited due to inherent technical problems, such as the installation challenges of encoders and IMU's drifting, acceleration, and magnetic issues. Thus, we propose a novel and reliable sensing system consisting of absolute rotary encoders and visual-inertial sensors for the upper-limb exoskeleton in VR therapy. Our sensing system has demonstrated angle measurement for various robot joint types, including hinge, ball, and revolute joints along the limb's longitudinal axis. Its sensing feedback can construct virtual arms that interact with virtual objects in the VR environment. In our experiments, with Vicon as the ground truth, our visual-inertial sensors achieved root-mean-square errors smaller than 2.3491° and a strong correlation ($r \geq 0.9640, p < 0.001$). Additionally, the experiment result of seven healthy subjects indicated that subjects had similar muscle activations, joint ROM, and joint trajectories in the VR task with our sensing system, compared with the real-world task. Thus, our proposed sensing system can potentially be used in the upper-limb exoskeleton for VR therapy.**

Keywords— Upper-limb exoskeleton, virtual reality (VR), rehabilitation robot, visual-inertial sensors, inertial measurement units (IMUs)

I. INTRODUCTION

Stroke is a neurological disease severely affecting patients' upper limb motor function. Around 80% of stroke patients have upper limb motor function impairment [1], and 69% of them cannot perform activities of daily living (ADL) independently [2]. In recent years, exoskeletons have been developed for stroke rehabilitation [3-5] because they have a higher potential to reduce therapists' workload and provide high-dosage, high-intensity, task-oriented, and consistent training. In addition, much literature has demonstrated that virtual reality (VR) technology can enhance robotic therapies [6, 7]; its engaging visual feedbacks enrich the training environment and promote motor learning [8].

Virtual reality (VR) is a powerful technology that provides a structured and safe environment for ADL training. Simulating ADL tasks in VR allows patients to experience similar real-world training [6] and transfer the trained skill to real-world scenarios. Further, the therapist can easily adjust task difficulties according to patients' capabilities, such as adjusting training goals and parameters like the size and position of objects. Besides, VR can guarantee safety in ADL training since it will not directly affect patients when they fail to complete the ADL task. For example, patients will not get injured when they fail ADL tasks like cooking, bread-cutting, and water-pouring. Moreover, much literature reported that VR could promote recovery in the arm's range of motion (ROM) [9], motor function [10, 11], and ADL function [6], improving patients' quality of life. Furthermore, VR or game-based training may have a better recovery outcome than conventional physical and occupational therapy by motivating patients to achieve more repetition of movement [12].

Unfortunately, the effectiveness of VR therapy is mainly limited by the sensing accuracy of exoskeletons. Their sensors can measure the real-time joint angles and arm positions for simulating virtual arms and interacting with the VR environment. However, sensing errors may confuse patients about their virtual arm's position, affecting their sense of presence in VR [13] and the virtual arm control. Besides, patients may not train the target muscle or motion with inaccurate visual feedback in VR; they may have different arm motions and muscle activation to compensate for the sensing error. Furthermore, the sensing error may affect the patient evaluation regarding joints' ROM and undesired compensatory movement during training. Such sensing errors are closely related to the sensor.

Most rehabilitation exoskeletons have a limited choice of sensors for joint angle measurements, particularly for the scapula, shoulder, or forearm. For example, (1) rotary encoder in ARMin [14] and ASSITON-SE [15]; and (2) inertial measurement unit (IMU) in cable-driven lower limb exoskeleton [16] and CAREX-7 [17]. Yet, encoders cannot measure spherical movements of shoulder joints and forearm rotation without additional mechanical structure, for instance, the Gimbal mechanism for spherical movements [18], as well as a timing-belt-pulley mechanism [19] and Harmony's forearm mechanism [20] for forearm rotation. These mechanical structures may be too bulky and impede the patients' motion. Furthermore, the IMU, a lighter and more convenient option, has inherent problems because the magnetometer is susceptible to a magnetic field near

ferromagnetic materials and electronic devices, the accelerometer is affected by the exoskeleton motion, and the gyroscope has an integration drift issue. Thus, IMU cannot provide a reliable angle measurement during long-hour robotic rehabilitation training. Nevertheless, there are more choices for joint angle measurement, e.g., depth camera [21, 22], flexible goniometer [23, 24], and visual-inertial sensors [25-27]. Although depth cameras and goniometers are unsuitable for exoskeletons due to low sensing frequency and mechanical limitation, visual-inertial sensors are promising because of their easy-to-install and magnetometer-free property. However, a limited exoskeleton has implemented the visual-inertial sensor to test its feasibility in robot joint measurement.

The current study aims to develop a reliable sensing system for measuring the joint angle of the upper limb exoskeleton in VR Therapy, providing a structured and safe environment for ADL training. This paper will demonstrate the angle measurement of various robot joint types, including hinge joints, ball joints, and revolute joints along the limb's longitudinal axis, with absolute rotary encoders and visual-inertial sensors. Besides, this sensing technique is easy-to-implement and transferable to other robots without any additional mechanical structures.

The rest of the paper is organized as follows. Section II describes the sensing requirements and proposed sensing system for joint measurement of the upper limb exoskeleton. Section III presents the experimental validation of the sensing system and an ADL task with seven healthy subjects. Finally, Section IV contains a discussion and potential research contributions.

II. Novel Approach to Exoskeleton Sensing

To train stroke patients in VR, the sensing system should fulfill two main requirements: (1) measure the joint movement for virtual arm construction and (2) detect hand grabbing for interacting with virtual objects.

As for robot joint measurement, measuring the ball joint and revolute joints along the limb's longitudinal axis is challenging. Since the Underactuated Upper Limb Exoskeleton (UULE) was used to demonstrate the sensing system in this paper, sensors for various joint types are needed. For example, as shown in Fig. 1, the UULE used three joint types: (1) a ball joint for scapula protraction/retraction motion (sP/R); (2) hinge joints for shoulder flexion/extension (sF/E), elbow flexion/extension (eF/E), and wrist flexion/extension (wF/E); and (3) revolute joints for shoulder internal/external rotation (sR) and forearm pronation/supination (eR). However, the rotary encoder can only measure hinge joints, not ball joints with three rotation axes or revolute joints along the limb's longitudinal axis. Also, as mentioned, IMU cannot provide a reliable global orientation for the exoskeleton, posing difficulty in synchronizing the motion of the exoskeleton and virtual arms. So, we applied novel visual-inertial sensors to provide the global orientations of ball joints and revolute joints.

During ADL training in VR, hand-grabbing detection is required for virtual object manipulation. Given that patients need to grab and manipulate the daily objects to perform the ADL, the VR ADL training should provide such grabbing motions allowing interaction between patients and the virtual environment. To detect hand grabbing, we installed a Force Sensing Resistor (FSR) sensor on the handle. The FSR detects the presence of finger-tip force when the patient grabs the handle. When exceeding a defined force threshold, the hand-grabbing motion is detected, allowing the patient to grab virtual objects in VR.

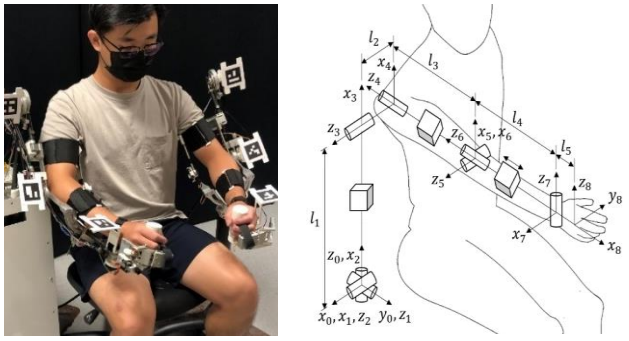

(a) (b)

Fig. 1. (a) The overview of the UULE exoskeleton worn by a subject. (b) The kinematic model.

A. Proposed Sensing System for Joint Measurement

To provide reliable global orientations of ball joints and revolute joints, the UULE used visual-inertial sensors. As shown in Fig. 2, a visual-inertial sensor consists of an IMU and camera system with Aruco markers. It fuses computer vision and IMU measurements, providing a more reliable global orientation. Specifically, computer vision measurement is complementary to IMU measurements (without using magnetometer data); measurement will not be stopped when missing the Aruco markers. However, it will have the same IMU drifting issue if missing the marker for an extended period. The detailed working principle and fusion algorithm can be found in our previous work [26, 28]. In brief, the monocular camera faces the user and robot, while the sensor modules are installed on the robots. The global pose of the ArUco markers can be detected from image processing using OpenCV. The transform of coordinate frames between the IMU and ArUco marker is precalibrated. Thus, the global orientation of the IMU-ArUco sensor module can be estimated with an extended Kalman filter (EKF) by fusing the raw accelerations, angular velocities, and marker pose. The orientations of the sensor module in quaternions are set as state variables of the EKF, and integration with the angular velocities from the process model. The accelerations and marker orientation are then set as the observations in the EKF. Since the image capture frequency is much lower than the IMU, the marker pose is only fused when available, while the accelerations are constantly fused. With the fused measurements, the orientation of IMU, expressed in quaternions, can be obtained and used in angle measurements of ball joints and revolute joints.

Regarding the ball joint for sP/R, the three rotations along axes (i.e., z_0, z_1, z_2) were measured by a visual-inertial sensor directly. As shown in Fig. 1(a) and Fig. 2, the sensor was installed at the robot's shoulder joint. After obtaining the sensor's orientation, the quaternions were converted to the ZYX Euler angle. Given that the global base frame was defined as $x_0 - y_0 - z_0$ coordinate, the ZYX Euler angles represented

the rotations (q_1, q_2, q_3) along z_0, y_0, and x_0 respectively. Although the conversion between quaternions to the Euler angle will have singularity when q_2 is 90° [29], the singularity will never occur because $q_2 < 90°$ when attaching the robot to human body. Hence, the ball joint's angles can be measured.

At the revolute joints along the limb's longitudinal axis, the rotation was measured by two visual-inertial sensors. Precisely, the q_5 for sR is the relative rotation of the visual-inertial sensors at the robot's shoulder (S1) and elbow joints (S2), while the q_7 for eR is the relative rotation of the sensors at the elbow (S2) and wrist joints (S3). After obtaining the sensors' orientations, the relative rotation (r) was computed as follows.

$$r = \theta_1^* \times \theta_2 \quad (1)$$

, where the '*' indicate the conjugate of quaternion and '×' is quaternion multiplication. For sR, r is the rotation of S2 relative to S1, while $\theta_1$and θ_2 are the quaternions obtained by S1 and S2, representing the rotations relative to the global base frame; for eR, r is S3 relative to S2, while $\theta_1$and θ_2 are the quaternions obtained by S2 and S3. After that, the relative rotation was converted to the ZYX Euler angle representation. So, the rotation of revolute joints along the limb's longitudinal axis can be measured.

Theoretically, the angle of sF/E (q_4) and eF/E (q_6) can be obtained during the computation. However, we apply the rotary encoders for sF/E and eF/E because they can be installed easily, as shown in Fig. 2, and achieve higher sensing frequencies while guaranteeing sensing accuracy, which benefits VR and robot control. Likewise, the angle of wF/E (q_8) is measured by a rotary encoder.

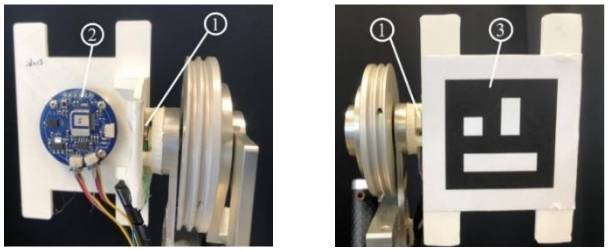

(a) (b)

Fig. 2. The sensors for sF/E and sP/R at the shoulder joint with (a) back view and (b) front view. The number indicates the sensors: (1) absolute rotary encoder for sF/E, (2) IMU of visual-inertial sensors for sP/R, and (3) Aruco marker of visual-inertial sensors.

B. Virtual Arm Construction for VR

The virtual limbs can be constructed in VR for Human-VR interaction after obtaining the reliable joint measurement of the robot or human limbs. We used a connected virtual limb in an arm shape to represent a limb in VR. In literature, there are three common limb representations in VR: virtual objects, a detached virtual arm, and a connected virtual arm. According to [30], virtual arms resembling real arms can develop users' body ownership; however, many existing game scenes used objects to represent the limb, e.g., the rectangular bar in the ball game [14] and a vehicle in the driving game [31]. Additionally, although some VR therapies used virtual arms, they used detached virtual forearms or hands, for instance, the 3D upper limb rehabilitation game for ADL [31]. As proved in [32], such detached hands negatively alter users' body ownership and arms control in VR, impacting the training outcome of VR therapy. Hence, a connected virtual arm was used.

Furthermore, the virtual arm's motion was controlled by Forward Kinematics (FK) with robot joint measurements. After constructing the virtual arm according to the D-H Table in Table. 1, we applied FK in Unity3D to control the arm motion.

Another challenge of virtual arm control is the translation of virtual arms. Since the scapula allows shoulder translation during upper limb motion, the virtual arm should simulate such translation because it can visualize the undesired shoulder compensatory movement [33], which is essential for patient evaluation. Besides, other joints' movements may differ when performing an ADL task without shoulder translation. However, limited VR simulated the shoulder translation because the robot did not mechanically support [34] or sense [35] shoulder translation. The UULE has a passive ball joint (sP/R) that conforms to shoulder translation. Given a long radius from the rotation axis, between sP/R and sF/E, and a small rotation angle ($|q_2| \leq 10°$ and $|q_3| \leq 10°$), the resulting movement of the ball joint can be approximated as a horizontal translation. And the horizontal translation along x (s_1) and y axes (s_2) can be calculated with the D-H table,

$$s = \begin{bmatrix} l_1 \sin(q_1)\sin(q_3) + l_1 \cos(q_1)\cos(q_3)\cos(q_2 - pi/2) \\ -l_1 cos(q_1) sin(q3) + l_1 cos(q_3) cos(q_2 - pi/2) sin(q_1) \\ -l_1 cos(q_3) sin(q_2 - pi/2) \end{bmatrix} \quad (2)$$

Note that the slight vertical offset (s_3) is induced by horizontal translation, which may not be the patients' intended movements. Nevertheless, the shoulder translation can be measured to translate the virtual arm.

TABLE 1
The D-H parameters of the UULE's kinematic model

	α_i	a_i	d_i	θ_i
0 - 1	$-\pi/2$	0	0	q_1
1 - 2	$-\pi/2$	0	0	$q_2 - \pi/2$
2 - 3	0	l_1	0	q_3
3 - 4	$-\pi/2$	0	$-l_2$	q_4
4 - 5	$\pi/2$	0	$-l_3$	q_5
5 - 6	$-\pi/2$	0	0	q_6
6 - 7	$-\pi/2$	0	$-l_4$	$q_7 - \pi/2$
7 - 8	0	l_5	0	$q_8 + \pi/2$

III. EXPERIMENT VALIDATION

A. Hardware of the Proposed Sensing System

The sensing system, including visual-inertial sensors and rotary encoders, was implemented in the PC/104, a real-time control system running Linux operating system with the real-time kernel patch (RT-Preempt). The visual-inertial sensors include a monocular camera, an Aruco marker (5cm x 5cm), and an IMU. The camera captured images (720 p/120 fps) at 10 Hz and sent them to PC/104 via serial port for the marker's orientation measurement. Then, the measurement was sent to the Teensy board (v4.0) for data fusion. As to the customized IMU module with sensor chip (BNO080, Bose, US), the inertial data was sampled at 100 Hz and sent to the Teensy board with Controller Area Network (CAN) protocol. Subsequently, the fused data from the Teensy board was sent to the PC/104 for calculating the angles of the ball and revolute

joints. Besides, the hinge joints' movements were measured by absolute rotary encoders (Renishaw RLS, RM08), as well as the hand motion was detected by 20mm x 20mm FSR and sent to PC/104 at 500 Hz. After that, the joint kinematic data was sent to a laptop running Unity3D via User Datagram Protocol (UDP) at 70 Hz, with 2.983ms of the UDP connection latency.

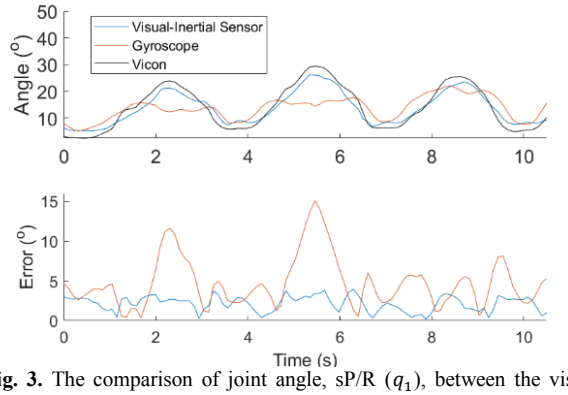

Fig. 3. The comparison of joint angle, sP/R (q_1), between the visual-inertial sensor and gyroscope.

B. Joint Measurement using Visual-inertial Sensors

The experiment is to validate the accuracy of visual-inertial sensors compared with the gyroscope of IMU. In this experiment, we can observe that the accuracy of visual-inertial sensors is better than the IMU, a commonly used sensor in existing robots. To compare them fairly, the accuracy of IMU is comparable to the IMU in [33]; a similar accuracy was achieved with a gyroscope in a short experiment period (< 11 s). Besides, the ground truth measurement was obtained by an eight-camera optical motion capture system (VICON, Oxford, UK).

Visual-inertial sensors can provide more reliable angle feedback with accurate amplitudes and shapes, as shown in Fig. 3. In the figure, the visual-inertial sensor maintained a small max error (<5°), while the gyroscope had errors exceeding 15°. Table 2 has further proved that visual-inertial sensors have smaller root-mean-square errors (RMSE) of joints than the gyroscope. The maximum RMSE of all joints was only 2.3491° and had a strong correlation with the ground truth ($r \geq 0.9832, p < 0.001$), while the gyroscope had 5.7080° maximum RMSE, with a weaker correlation ($r \leq 0.7353, p < 0.001$). In addition, the errors of our visual-inertial sensors are comparable with another visual-inertial sensor (RMSE 2.7° with correlation 0.87) in [25], as well as more minor than other IMU (RMSE 5.6°) in [36] and IMU (4° of median error) in [33].

Likewise, a higher accuracy of visual-inertial sensors can be observed in shoulder translation, shown in Table 3. Since the shoulder translation was computed with Eqn. (2) and joint feedback (q_1, q_2, q_3), sensors with more accurate angle feedback can provide more reliable position feedback of the shoulder. The maximum RMSE was 7.7097mm, sufficient in VR and rehabilitation training since they are far smaller than 5cm of the compensatory detection requirement [33].

Hence, visual-inertial sensors can provide higher accuracy of joint angle feedback for VR than the existing method with IMU. However, we do not know whether the accuracy is sufficient to provide a similar training environment as the real world.

TABLE 2
The comparison of joint angles between the visual-inertial sensor and gyroscope

	Visual-inertial Sensor		**Gyroscope (IMU)**	
	RMSE (°)	**Pearson Correlation Coefficient ($p < 0.001$)**	**RMSE (°)**	**Pearson Correlation Coefficient ($p < 0.001$)**
sP/R (q_1)	2.3491	0.9832	5.7080	0.7353
sP/R (q_2)	1.0335	0.9640	1.8440	0.7003
sP/R (q_3)	0.7247	0.9978	4.3427	0.9648
sR (q_5)	2.0742	0.9978	4.1918	0.9985
eR (q_7)	2.2133	0.9990	5.4026	0.9992

TABLE 3
The comparison of shoulder translation between the visual-inertial sensor and gyroscope

	Visual-inertial Sensor		**Gyroscope (IMU)**	
	RMSE (mm)	**Pearson Correlation Coefficient ($p < 0.001$)**	**RMSE (mm)**	**Pearson Correlation Coefficient ($p < 0.001$)**
sP/R (x)	7.7097	0.7842	15.5894	0.4218
sP/R (y)	4.6597	0.9978	22.3897	0.9676
sP/R (z)	0.6808	0.9939	4.6876	0.8662

C. Evaluation with an ADL Task

The sensing system was evaluated on seven healthy subjects A-G (four females and three males, ages 21-45) who were staff or students at the university. All participants provided informed consent before participation, and the protocols were approved by the Institutional Review Board (IRB) of the National University of Singapore (NUS) under IRB approval No. (NUS-IRB-2022-337).

The experiment aims to test the hypothesis that with the small kinematic sensing error in VR, subjects can still perform a virtual ADL task with (1) muscle activation, (2) joint ROM, and (3) joint trajectories similar to a real-world task. Although the sensing system has minor errors in joints' measurements, their effect on human motion in VR is unknown. Hence, it is challenging to predict the effectiveness of the proposed sensing system in future VR therapy. It is necessary to prove that subjects can perform similarly in VR. In the experiment, subjects performed a burger-transferring task by grabbing the burger in a fixed location and transferring it to their mouth. The subjects performed the task three times in each experimental condition: VR and the real world. The experiment setups in both conditions are shown in Fig. 4. During the experiment, (1) the subject relaxed and started at 0% of the motion cycle, (2) flexed his/her elbow and approached the burger at 30% motion cycle, (3) grabbed the burger at 70% of the motion cycle, and (4) transferred the burger to his/her mouth at 100% motion cycle. After analysis, three main results can be obtained.

Firstly, the tendency of muscle activation in VR was similar to the real world in the motion cycle. To measure muscle activation, we used eight EMG sensors (Delsys Trigno Avanti Sensor, sampling rate of 2150 Hz) and placed them on the subject's right arm, as shown in Fig 5. Table. 4 shows the relationship between joint motions, muscles, and the EMG sensors. Before analysis, each EMG signal

was rectified and filtered with a second-order bandpass Butterworth filter with bandwidth 6-800 Hz, smoothened by the moving average with 0.2s of window size, and normalized to subjects' maximum voluntary contraction (MVC). After that, as shown in Fig. 6, subject A had a similar EMG tendency in both VR and the real world. Further, such similarity was observed in seven subjects in Fig. 7 (a). The seven subjects' averaged EMG in three repetitions showed no statistically significant difference for all muscles, assessed by the Wilcoxon signed rank test, and a strong correlation ($\rho \geq 0.821, p < 0.05$) with Spearman's rank correlation for most of the muscles. Although Ch. 6 (Supinator) did not show the correlation statistically, a similar tendency can be observed.

Secondly, the joint ROM in VR was similar to the real world. As shown in Fig. 7 (b), with joint angle feedback of the sensing system, all seven subjects' averaged joint ROM in three repetitions indicated no statistically significant difference in Wilcoxon signed rank test. Also, most of the joints, except q_7 and q_8, exhibited a strong Spearman's rank correlation ($\rho \geq 0.786, p < 0.05$). But still, a similar joint ROM of q_7 and q_8 can be observed in the figure.

Thirdly, the joint trajectories in VR were similar to the real world. Fig. 7 shows that subject A had similar joint trajectories (q_4, q_6, q_7 , q_8) in the motion cycle. Moreover, when comparing all the averaged joint trajectories of seven subjects in three repetitions under VR and real-world conditions, most of the joints except q_5 and q_7 had a strong Pearson correlation ($r \geq 0.8179, p < 0.01$), shown in Table 5. The weak-to-moderate Pearson correlation of q_5 ($r = 0.3008 \pm 0.4717, p < 0.01$) and q_7 ($r = 0.2247 \pm 0.5330, p < 0.01$) may be attributed to the reasons that the burger-transferring ADL task mainly requires elbow movements (q_6), shown in Fig. 7 (b), and minor orientation differences of the virtual hand will not significantly affect the burger-grabbing motion. Despite the weak-to-moderate Pearson correlation of these two joints, all joints had no statistically significant difference in Student's t-test and had small RMSE (average $\leq 9.3523°$), showing similar joint trajectories in VR and the real world.

So, the experiment can preliminarily show that the small sensing error will not significantly affect human motion in VR in terms of (1) muscle activation, (2) joint ROM, and (3) joint trajectories; a similar ADL motion can potentially be trained in virtual ADL training with our sensing system. However, more human experiments should be conducted to confirm this result further.

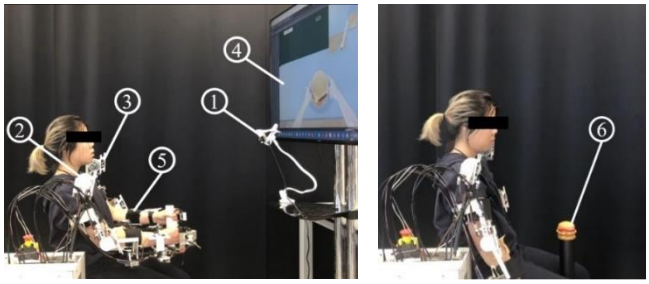

(a) (b)

Fig. 4. Experiment setup for (a) VR and (b) the real world. The number indicates the devices: (1) camera, (2) IMU, (3) Aruco marker, (4) monitor for visual feedback, (5) UULE, and (6) toy burger.

TABLE 4
The relationship between the motion, muscles, and EMG sensors

Motion of joint	**Muscle**	**EMG**
Shoulder flexion	Anterior deltoid	Ch. 1
Shoulder extension	Posterior deltoid	Ch. 2
Elbow flexion	Biceps	Ch. 3
Elbow extension	Triceps	Ch. 4
Forearm pronation	Pronator teres	Ch. 5
Forearm supination	Supinator	Ch. 6
Wrist flexion	Flexor carpi radialis (FCR)	Ch. 7
Wrist extension	Extensor carpi radialis brevis (ECRB)	Ch. 8

Fig. 5. The EMG placement on a healthy subject.

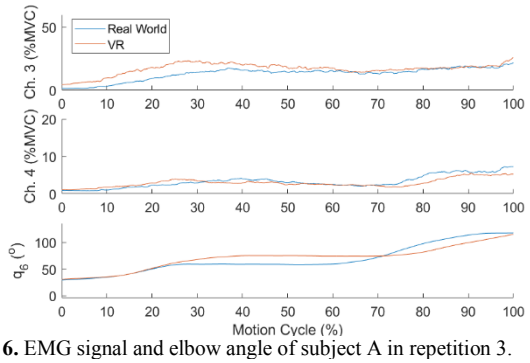

Fig. 6. EMG signal and elbow angle of subject A in repetition 3.

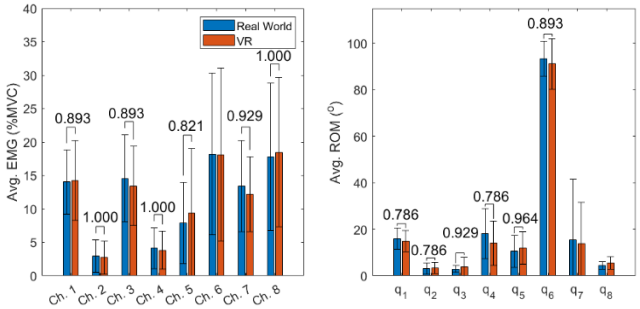

(a) (b)

Fig. 7. (a) The average EMG signal and (b) the average ROM of seven subjects. The numbers represent Spearman's Rho (ρ).

TABLE 5
The average error and correlation of subjects' joint trajectories between VR and the real world

	RMSE (°) (mean $\pm$ sd)	**Pearson Correlation Coefficient** (mean $\pm$ sd) ($p < 0.01$)
sP/R (q_1)	2.6415 $\pm$ 3.4470	0.9381 $\pm$ 0.0415
sP/R (q_2)	0.6974 $\pm$ 0.4902	0.8764 $\pm$ 0.1166
sP/R (q_3)	0.8299 $\pm$ 0.7486	0.8210 $\pm$ 0.0829
sF/E (q_4)	4.2284 $\pm$ 2.5656	0.8179 $\pm$ 0.1180
sR (q_5)	5.9244 $\pm$ 4.3689	0.3008 $\pm$ 0.4717
eF/E (q_6)	9.3523 $\pm$ 5.7084	0.9432 $\pm$ 0.0333
eR (q_7)	4.9317 $\pm$ 5.3524	0.2247 $\pm$ 0.5330
wF/E (q_8)	3.5305 $\pm$ 4.9639	0.8800 $\pm$ 0.0924

IV. Discussion

A limited robot sensing system is proven reliable to provide a similar virtual environment for rehabilitation training. As we know, VR can be so helpful in rehabilitation training that it can provide a safe and structured environment for rehabilitation training. However, the current robot sensors like rotary encoder and IMU will limit their effectiveness. Moreover, limited research studies can show that the small sensing error of their sensors will not confuse patients and change their movement during VR therapy; hence, we cannot conclude that the current sensors can provide reliable kinematic feedback for VR therapy.

Thus, a novel and reliable sensing system is proposed for robotic therapy with VR technology. The proposed sensing system measured the angles of various robot joint types, including hinge, ball, and revolute joints along the limb's longitudinal axis, with absolute rotary encoders and visual-inertial sensors. The sensing feedback can construct the virtual arm movement and interact with virtual objects in the VR environment. In experiments, visual-inertial sensors were proven to provide more accurate angle feedback than the gyroscope of IMU, and the errors of visual-inertial sensors are comparable with the visual-inertial sensor in [25] and smaller than the IMU in [33, 36]. This can demonstrate the use and accuracy of visual-inertial sensors in exoskeleton applications, while limited literature has implemented such a sensor in robots.

Further, with our proposed sensing system, seven subjects showed limited effects of VR on muscle activations, joint ROM, and joint trajectories, indicating that the proposed sensing system is reliable and accurate enough for reconstructing real-world ADL training in VR. These results imply the excellent potential for such a sensing system in robotic and VR therapy by providing a safe, structured rehabilitation training environment that therapists fully control. Moreover, such results are transferable to other robot devices.

Additionally, joint measurement can be used in patient assessment. Since robot joints align with patients' joints, their joint trajectories or ROM can be estimated by the robot joint movements. So, such joint trajectories can be used to evaluate patients' joint impairments and monitor their recovery. Moreover, shoulder translation can be measured for assessing shoulder compensatory movement during ADL training, which can show whether patients have learned bad-use that impedes their recovery, e.g., decreased ROMs of the shoulder and elbow joint that are compensated by excessive trunk movement and shoulder translation [37-39].

References

[1] H. Rodgers *et al.*, "Robot assisted training for the upper limb after stroke (RATULS): a multicentre randomised controlled trial," *The Lancet,* vol. 394, no. 10192, pp. 51-62, 2019.

[2] H. Nakayama, H. S. Jorgensen, H. O. Raaschou, and T. S. Olsen, "Recovery of upper extremity function in stroke patients: the Copenhagen Stroke Study," *Arch Phys Med Rehabil,* vol. 75, no. 4, pp. 394-8, 1994.

[3] G. Bao *et al.*, "Academic Review and Perspectives on Robotic Exoskeletons," *IEEE Transactions on Neural Systems and Rehabilitation Engineering,* vol. 27, no. 11, pp. 2294-2304, 2019.

[4] F. Molteni, G. Gasperini, G. Cannaviello, and E. Guanziroli, "Exoskeleton and End-Effector Robots for Upper and Lower Limbs Rehabilitation: Narrative Review," *PM&R,* vol. 10, no. 9S2, pp. S174-S188, 2018.

[5] S. H. Lee *et al.*, "Comparisons between end-effector and exoskeleton rehabilitation robots regarding upper extremity function among chronic stroke patients with moderate-to-severe upper limb impairment," *Scientific Reports,* vol. 10, no. 1, p. 1806, 2020.

[6] X. Chen, F. Liu, S. Lin, L. Yu, and R. Lin, "Effects of Virtual Reality Rehabilitation Training on Cognitive Function and Activities of Daily Living of Patients With Poststroke Cognitive Impairment: A Systematic Review and Meta-Analysis," *Archives of Physical Medicine and Rehabilitation,* vol. 103, no. 7, pp. 1422-1435, 2022.

[7] D. Jack *et al.*, "Virtual reality-enhanced stroke rehabilitation," *IEEE Transactions on Neural Systems and Rehabilitation Engineering,* vol. 9, no. 3, pp. 308-318, 2001.

[8] M. Levin, P. Weiss, and E. Keshner, "Emergence of Virtual Reality as a Tool for Upper Limb Rehabilitation," *Physical therapy,* 2014.

[9] A. V. Soares, S. S. Woellner, C. d. S. Andrade, T. J. Mesadri, A. D. Bruckheimer, and M. d. S. Hounsell, "The use of Virtual Reality for upper limb rehabilitation of hemiparetic Stroke patients," *Fisioterapia em Movimento,* vol. 27, pp. 309-317, 2014.

[10] P. Domínguez-Téllez, J. A. Moral-Muñoz, A. Salazar, E. Casado-Fernández, and D. Lucena-Antón, "Game-Based Virtual Reality Interventions to Improve Upper Limb Motor Function and Quality of Life After Stroke: Systematic Review and Meta-analysis," *Games for Health Journal,* vol. 9, no. 1, pp. 1-10, 2020.

[11] M. Park *et al.*, "Effects of virtual reality-based planar motion exercises on upper extremity function, range of motion, and health-related quality of life: a multicenter, single-blinded, randomized, controlled pilot study," *Journal of NeuroEngineering and Rehabilitation,* vol. 16, no. 1, p. 122, 2019.

[12] R. Karamians, R. Proffitt, D. Kline, and L. V. Gauthier, "Effectiveness of Virtual Reality- and Gaming-Based Interventions for Upper Extremity Rehabilitation Poststroke: A Meta-analysis," *Archives of Physical Medicine and Rehabilitation,* vol. 101, no. 5, pp. 885-896, 2020.

[13] H. Si-Mohammed *et al.*, "Detecting System Errors in Virtual Reality Using EEG Through Error-Related Potentials," in *2020 IEEE Conference on Virtual Reality and 3D User Interfaces (VR)*, 2020, pp. 653-661.

[14] T. Nef, M. Mihelj, and R. Riener, "ARMin: a robot for patient-cooperative arm therapy," *Medical & Biological Engineering & Computing,* vol. 45, no. 9, pp. 887-900, 2007.

[15] M. A. Ergin and V. Patoglu, "ASSISTON-SE: A self-aligning shoulder-elbow exoskeleton," in *2012 IEEE International Conference on Robotics and Automation*, 2012, pp. 2479-2485.

[16] B. Zhong, K. Guo, H. Yu, and M. Zhang, "Toward Gait Symmetry Enhancement via a Cable-Driven Exoskeleton Powered by Series Elastic Actuators," *IEEE Robotics and Automation Letters,* vol. 7, no. 2, pp. 786-793, 2022.

[17] X. Cui, W. Chen, X. Jin, and S. K. Agrawal, "Design of a 7-DOF Cable-Driven Arm Exoskeleton (CAREX-7) and a Controller for Dexterous Motion Training or Assistance," *IEEE/ASME Transactions on Mechatronics,* vol. 22, no. 1, pp. 161-172, 2017.

[18] R. Soltani-Zarrin, A. Zeiaee, A. Eib, R. Langari, N. Robson, and R. Tafreshi, "TAMU CLEVERarm: A novel exoskeleton for rehabilitation of upper limb impairments," in *2017 International Symposium on Wearable Robotics and Rehabilitation (WeRob)*, 2017, pp. 1-2.

[19] T. Nef, M. Mihelj, G. Kiefer, C. Perndl, R. Muller, and R. Riener, "ARMin - Exoskeleton for Arm Therapy in Stroke Patients," in *2007 IEEE 10th International Conference on Rehabilitation Robotics*, 2007, pp. 68-74.

[20] B. Kim and A. D. Deshpande, "An upper-body rehabilitation exoskeleton Harmony with an anatomical shoulder mechanism: Design, modeling, control, and performance evaluation," *The International Journal of Robotics Research,* vol. 36, no. 4, pp. 414-435, 2017.

[21] Z. Moore, C. Sifferman, S. Tullis, M. Ma, R. Proffitt, and M. Skubic, "Depth Sensor-Based In-Home Daily Activity Recognition and Assessment System for Stroke Rehabilitation," in *2019 IEEE*

International Conference on Bioinformatics and Biomedicine (BIBM), 2019, pp. 1051-1056.

[22] M. Elgendi, F. Picon, N. Thalmann, and D. Abbott, "Arm movement speed assessment via a Kinect camera: A preliminary study in healthy subjects," *BioMedical Engineering OnLine,* vol. 13, 2014.

[23] A. Tognetti, F. Lorussi, N. Carbonaro, and D. De Rossi, "Wearable Goniometer and Accelerometer Sensory Fusion for Knee Joint Angle Measurement in Daily Life," *Sensors*, vol. 15, no. 11, pp. 28435-28455.

[24] H. Hayashi and H. Shimizu, "Essential motion of metacarpophalangeal joints during activities of daily living," *Journal of Hand Therapy,* vol. 26, no. 1, pp. 69-74, 2013.

[25] R. Mallat, V. Bonnet, M. A. Khalil, and S. Mohammed, "Upper Limbs Kinematics Estimation Using Affordable Visual-Inertial Sensors," *IEEE Transactions on Automation Science and Engineering,* pp. 1-11, 2020.

[26] T. Li, X. Wu, H. Dong, and H. Yu, "Estimation of Upper Limb Kinematics with a Magnetometer-Free Egocentric Visual-Inertial System," in *2022 International Conference on Robotics and Automation (ICRA)*, 2022, pp. 1668-1674.

[27] Y. Lee, W. Do, H. Yoon, J. Heo, W. Lee, and D. Lee, "Visual-inertial hand motion tracking with robustness against occlusion, interference, and contact," *Science Robotics,* vol. 6, no. 58, p. eabe1315, 2021.

[28] T. Li, T. M. Kwok, X. Wu, S. Ding, and H. Yu, "Visual-Inertial Sensor System for Robot-Assisted Upper Limb Rehabilitation," in *IEEE Int. Conf. Adv. Robot. Mechatron.*, 2023.

[29] C. W. Kang and C. G. Park, "Euler Angle Based Attitude Estimation Avoiding the Singularity Problem," *IFAC Proceedings Volumes,* vol. 44, no. 1, pp. 2096-2102, 2011.

[30] M. Pyasik, G. Tieri, and L. Pia, "Visual appearance of the virtual hand affects embodiment in the virtual hand illusion," *Scientific Reports,* vol. 10, no. 1, p. 5412, 2020.

[31] G. Jin, K. Jiang, and S. Lee, "Development of Virtual Reality Games for Motor Rehabilitation," *Journal of Telecommunication, Electronic and Computer Engineering,* vol. 10, pp. 87-94, 2018.

[32] S. Seinfeld and J. Müller, "Impact of visuomotor feedback on the embodiment of virtual hands detached from the body," *Scientific Reports,* vol. 10, no. 1, p. 22427, 2020.

[33] A. Passon, T. Schauer, and T. Seel, "Inertial-Robotic Motion Tracking in End-Effector-Based Rehabilitation Robots," (in English), *Frontiers in Robotics and AI,* vol. 7, no. 167, 2020.

[34] L. I. Lugo-Villeda, A. Frisoli, E. Sotgiu, G. Greco, and M. Bergamasco, "Clinical VR applications with the light-exoskeleton for upper-part neurorehabilitation," in *19th International Symposium in Robot and Human Interactive Communication*, 2010, pp. 1-6.

[35] M. A. Gull *et al.*, "A 4-DOF Upper Limb Exoskeleton for Physical Assistance: Design, Modeling, Control and Performance Evaluation," *Applied Sciences,* vol. 11, no. 13, p. 5865, 2021.

[36] P. Slade, A. Habib, J. L. Hicks, and S. L. Delp, "An Open-Source and Wearable System for Measuring 3D Human Motion in Real-Time," *IEEE Transactions on Biomedical Engineering,* vol. 69, no. 2, pp. 678-688, 2022.

[37] W. Liu, S. McCombe Waller, T. M. Kepple, and J. Whitall, "Compensatory arm reaching strategies after stroke: induced position analysis," (in eng), *Journal of rehabilitation research and development,* vol. 50, no. 1, pp. 71-84, 2013.

[38] F. Grimm, G. Naros, and A. Gharabaghi, "Compensation or Restoration: Closed-Loop Feedback of Movement Quality for Assisted Reach-to-Grasp Exercises with a Multi-Joint Arm Exoskeleton," (in English), *Frontiers in Neuroscience,* vol. 10, 2016.

[39] M. F. Levin, D. G. Liebermann, Y. Parmet, and S. Berman, "Compensatory Versus Noncompensatory Shoulder Movements Used for Reaching in Stroke," *Neurorehabilitation and Neural Repair,* vol. 30, no. 7, pp. 635-646, 2015.